ACTA MECHANICA SINICA (English Series), Vol.13, No.4, Nov. 1997 ISSN 0567-7718
The Chinese Society of Theoretical and Applied Mechanics
Chinese Journal of Mechanics Press, Beijing, China
Allerton Press, INC., New York, U.S.A.

MOLECULAR DYNAMICS SIMULATIONS OF DFZ*

Zhou Guohui (周国辉) Lu Hong (吕 宏) Wan Farong (万发荣) Chu Wuyang (褚武扬)
(*Department of Materials Physics, University of Science and Technology of Beijing, Beijing* 100083, *China*)

Zhou Fuxin (周富信)
(*Institute of Mechanics, Chinese Academy of Sciences, Beijing* 100080, *China*)

ABSTRACT: Dislocation emission from the crack tip in copper under mode II loading is simulated with molecular dynamics method. After 26 partial dislocations are emitted and then relaxed to reach the equilibrium under the constant displacement, the double pile-ups (including an inverse pile-up and a pile-up) are formed. i.e., the first dislocation is piled up before the obstruction, and the last dislocation is piled up ahead of the crack tip. These results conform to the TEM observations.

KEY WORDS: copper, molecular dynamics simulation, DFZ

1 INTRODUCTION

Rice et al. considered that if dislocation emission was easier than cleavage, the crack would be blunted and the ductile fracture happened[1,2]. Otherwise, the brittle fracture happened. But the *in situ* observations showed that to both ductile and brittle materials, when loaded, dislocations would be emitted from the crack tip, and under the constant displacement, dislocations emitted would be piled up ahead of the crack tip and dislocation free zone (DFZ) would be formed. DFZ is an elastic zone, probably with very high stress level. As the DFZ is thinned heterogeneously, the stress in DFZ will probably reach atomic bond strength, resulting in the formation of nanocracks. To ductile materials[3], nanocracks will be quickly blunted into holes and notches. To brittle materials[4,5], nanocracks will propagate by cleavage. So, dislocation emission is the prerequisite for crack nucleation (or crack propagation) and the DFZ plays a key role in the nucleation of a microcrack.

To a mode II crack in a single crystal, after a serials of dislocations are emitted from a crack tip, the force which is acted on the i-th dislocation X_i is[6]

$$F_i = \frac{K_{II}b}{\sqrt{2\pi X_i}} - \frac{\mu b^2}{4\pi X_i(1-\nu)} + \sum_{j(j\neq i)} \frac{\mu b^2}{4\pi}\left(\frac{1}{X_i+\sqrt{X_iX_j}} + \frac{1}{X_j - X_i}\right) - b\tau_f \qquad (1)$$

where the first item on the right hand is the crack stress field, the second is the image force of the dislocation, the third is the interactive force between dislocations, and the last is lattice resistance. Keeping constant displacement after many dislocations are emitted, the

Received 14 October 1996
* The project supported by the National Natural Science Foundation of China

equilibrium is reached, then the force acted on each dislocation is equal to zero, i.e. $\Sigma F_i = 0$. From Eq.(1) we can calculate the distance of every dislocation departed from the crack tip. The calculation shows that dislocations are piled up inversely ahead of the crack tip. There is no dislocation in the zone between the crack tip and the last dislocation of the inverse pile-up, which is called dislocation free zone (DFZ)[7]. Many experiments have proved the existence of the DFZ[3~5,7]. In crystals, both second phase particles and grain boundaries are strong obstacles to dislocations. If a series of dislocations are emitted from the crack tip, advanced dislocations will be piled up ahead of these obstacles. In this case, an additional force which will be acted on each dislocation due to obstacles must be added in Eq.(1)

$$\frac{\mu b^2 \eta}{4\pi}\left(\frac{1}{X_i + \sqrt{X_i X_D}} + \frac{1}{X_D - X_i}\right) \tag{2}$$

Here X_D is the position of the obstacle, η is the intensity of the obstacle[6]. Under this condition, if constant displacement is kept, double pile-ups will be formed if the configuration reaches equilibrium. Our recent experiment proved it, see Fig.1. Figure 1 shows that there exist the inverse pile-up and pile-up at the same time. The first dislocation is obstructed ahead of the obstacle P, and this series of dislocations are inversely piled up before the crack tip A. Here AB is just the DFZ.

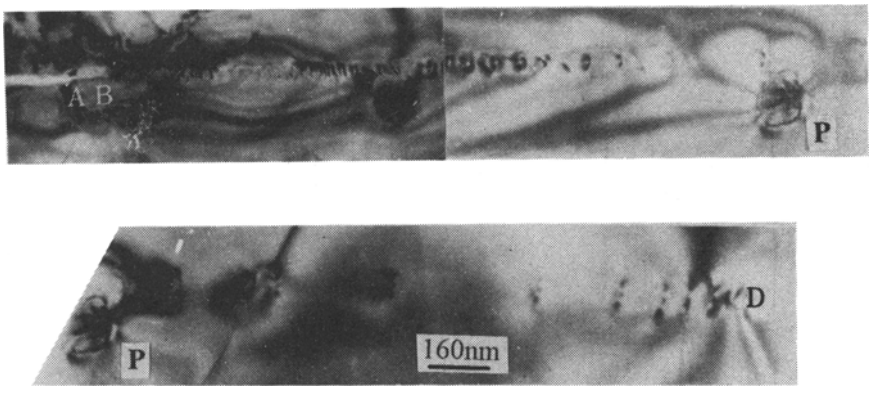

Fig.1 The atomic configuration of the inverse pile-up and pile-up after dislocations emitted from the crack tip reach the equilibrium. A is the crack tip, AB is DFZ, D is the second phase particle

Atomistic simulations on dislocation emission, formation of DFZ and nucleation of nanocracks with molecular dynamics simulation method are useful. However, influenced by Rice's ductile-brittle transition criterion, so far, all molecular dynamics simulations are limited in the competition between dislocation emission and bond breaking[8~10], and few people paid much attention on DFZ and the formation of nanocracks in DFZ. Maybe the reason is that the number of atoms involved in computation is few, and dislocations emitted is few. Moreover, if constant displacement is not kept after a series of dislocations are emitted, the equilibrium can not be obtained, so DFZ is not observed during the former computations. First at all, we simulate the formation of DFZ with molecular dynamics simulation method.

2 COMPUTATION PROCEDURE

The interatomic potential used here is the "N-body" potential proposed by Finnis and Sinclair[11] and constructed by Ackland et al.[12]. The ansatz they used is

$$U = -\sum_i \rho_i^{1/2} + \frac{1}{2}\sum_i \sum_{i(i\neq j)} V_{ij} \tag{3}$$

ρ is the second moment of the density of states, and

$$\rho_i = \sum_{j(i\neq j)} \Phi_{ij} \tag{4}$$

V_{ij} and Φ_{ij} are functions only of the interatomic distance, and can be obtained by assuming some functional forms and then fitting to the experimental data.

The {110}, {111} and {112} crystallographic planes of the parallelepiped with a slit are used in the present calculations. The coordinate system is selected to be x, y, z axes along ⟨110⟩, ⟨112⟩ and ⟨111⟩ directions respectively. In the FCC crystal, a full dislocation moves in the ⟨110⟩ direction in {111} plane. So, in the present model, the crack plane is taken to be in the {111} plane, and the crack front is along the ⟨112⟩ direction. The periodicity is in three layers along ⟨111⟩, two layers along ⟨110⟩ and six layers along ⟨112⟩. There are 44 periods along z direction, 132 layers, 928 periods along x direction, 1856 layers, and the length of the crystal is $w = 237\,\text{nm}$; along y direction 1 period, 6 layers. The total atomic number is $n = 2.44 \times 10^5$. The length of the crack is $a = 30.7\,\text{nm}$, and width is 0.63 nm. The ratio $a/w = 0.13$, and the ratio of length to width of the crack is 49. As the distance from the crack tip to the right boundary is large enough, the effect of the boundary constraints on the nucleation and emission of dislocations can be neglected if the dislocations are far from the boundary.

In the present simulations, a mode II loading is used, and the loading rate is $\mathrm{d}K_{II}/\mathrm{d}t = 0.08\text{MPa}\,\text{m}^{1/2}\text{ps}^{-1}$. The boundary conditions applied to the boundary of the discrete atom region in our molecular dynamics simulation have been that of a prescribed displacement distribution dictated by a mode II anisotropic K field in the x-z plane. Here the plane strain condition is used, i.e. $\varepsilon_{yy} = 0$. The inner atoms follow law of Newton, and the Leapfrog Algorithm[13] is applied to calculate positions and velocities of atoms. The time step is 2×10^{-14}s, the initial temperature is 40K. The initial velocity is the Maxwell-Boltzmann distribution corresponding to a given temperature. The temperature of the model is maintained to a constant value during simulations.

3 SIMULATED RESULTS

When external load is acted on the model, at the 320-th time step, the first partial dislocation is emitted from the crack tip, as shown in Fig.2(a). That is to say that the critical stress intensity factor for partial dislocation emission is $K_{IIe} = 0.512\,\text{MPa}\,\text{m}^{1/2}$. It should be pointed out that stress intensity factor K_{IIe} has a close relation with the loading rate, crack orientation and length. For example, keeping the loading rate constant, if the crack length is reduced from 30.7 nm to 2.56 nm, K_{IIe} declines to $0.22\text{MPa}\,\text{m}^{1/2}$. If the crack length is set to be 2.56 nm, and the loading rate declines from 0.08 to 0.005 $\text{MPa}\,\text{m}^{1/2}$, K_{IIe} declines from 0.22 to 0.18 $\text{MPa}\,\text{m}^{1/2}$. When the stress intensity factor K_{IIe} increases up

to 0.576 MPa$\sqrt{\text{m}}$, the second dislocation appears. Between two partial dislocations there is the stacking fault, and the stacking fault causes the energy of the crystal to increase, so almost all emitted dislocations appear in pairs, as shown in Fig.3. Near the boundary the separation of two partial dislocations is very small, and the separation of two full dislocations is also small. But to dislocations in the middle, the case is just opposite. The width of stacking fault is dependent not only on stacking fault energy but also on loading rate and stress fields where dislocations are located. At the 500-th time step, K_{IIe}=0.8 MPa$\sqrt{\text{m}}$, six partial dislocations have been emitted, as shown in Fig.2. The first emitted dislocation moves ahead approximately at the velocity of 2583 m/s, which is below the longitudinal wave speed of 4 560 m/s for copper. When it encounters the boundary, it slows down and is piled up.

At the 1000-th time step, K_{IIe}=1.6 MPa$\sqrt{\text{m}}$, 26 partial dislocations have been

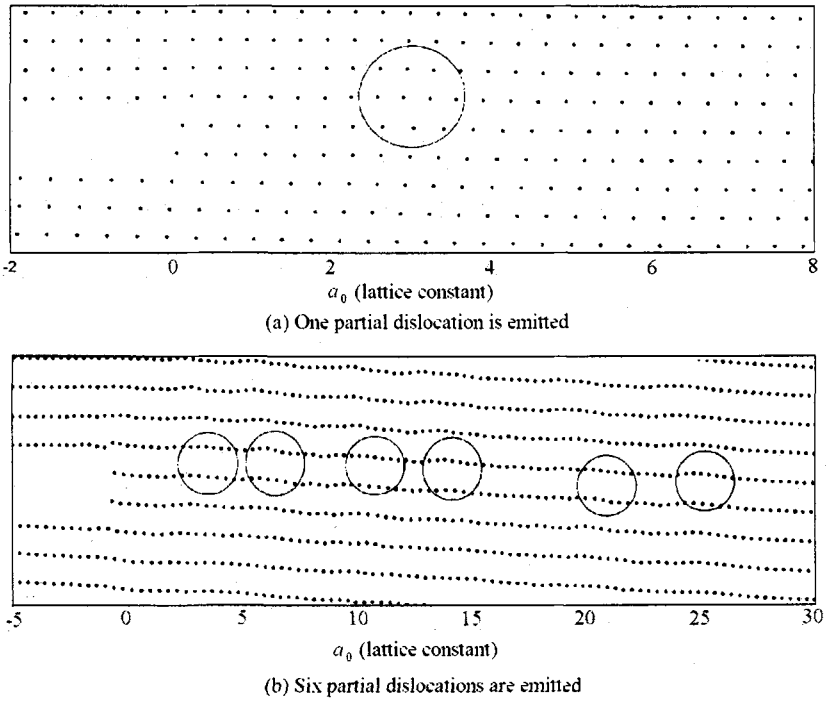

(a) One partial dislocation is emitted

(b) Six partial dislocations are emitted

Fig.2 The atomic configuration after partial dislocations are emitted from the crack tip

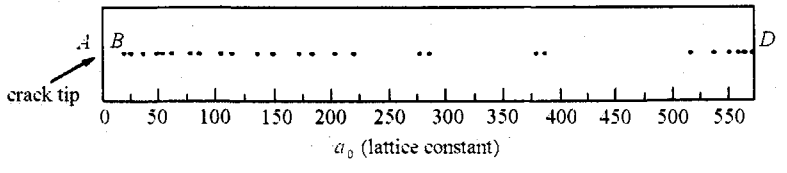

Fig.3 The positions of partial dislocations after 26 partial dislocations are emitted from the crack tip after equilibrium. A is the crack tip, D is the boundary, AB is DFZ

emitted from the crack tip. Keeping K_{IIe}=1.6 MPa m$^{1/2}$ constant, we relax the configuration until it reaches equilibrium. If the resultant of forces acted on each dislocation is zero, equilibrium is obtained, as shown in Fig.4. Ahead of the crack tip, dislocations are piled up inversely. The farther the dislocation is departed from the crack tip, the wider the distance between two full dislocations is, and AB is the DFZ. At the same time, dislocations are piled up in front of the obstacle. The double pile-ups conform with our experimental result very well (see Fig.1). Figure 4 is the equilibrium atomic configuration corresponding to Fig.3. In Fig.4(a) there exists a zone where there is no dislocation, we call it DFZ. From Fig.4(a), it is clearly known that the width of DFZ is about 7 nm. Figure 4(b) is the atomic configuration near the boundary. Four partial dislocations are piled up ahead of the boundary.

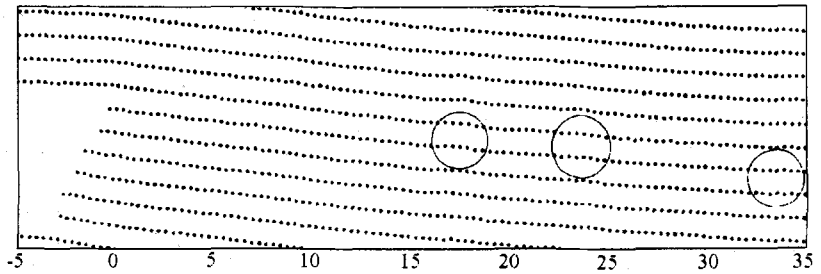

(a) The crack tip and the atomic configuration of the front 3 partial dislocations

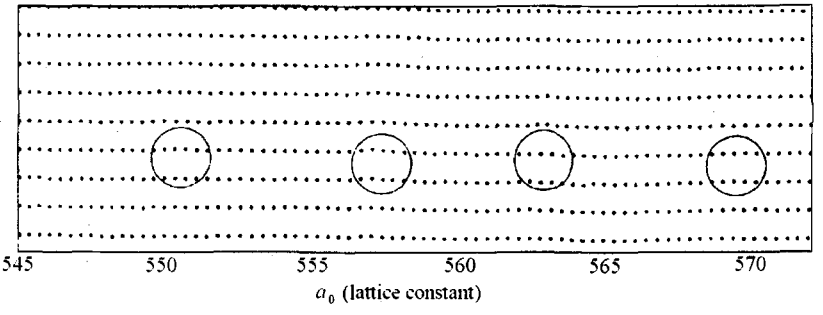

(b) The boundary and the atomic configuration of the last 4 partial dislocations

Fig.4 The equilibriom atomic configuration corresponding to Fig.3

4 CONCLUSIONS

The critical stress intensity factor K_{IIe} is associated with the loading rate and the length of the crack tip. The higher the loading rate, the higher the K_{IIe} will be. The separations of two partial dislocations and two full dislocations depend on stress of the area where they locate. If there are enough dislocations emitted , after reaching equilibrium, double pile-ups will be formed between the crack tip and the boundary (or particles). In the meanwhile, a DFZ is generated ahead of the crack tip. The computational results conform to the experiments.

Acknowledgement The author thanks Dr. Zhang Yongwei of Institute of Mechanics, Chinese Academy of Sciences for his help.

REFERENCES

1 Rice JR, Thomson R. Ductile versus brittle behaviour of crystals. *Phil Mag*, 1974, 29: 73~97

2 Beltz GE, Rice JR. Dislocation nucleation versus cleavage decohesion at crack tips. In: Modeling the Deformation of Crystalline Solids, presented at the Annual Meeting of the Minerals, Metals, and Materials Society, New Orleans, LA, USA, Feb. 17~21, 1991. Publ by Minerals, Metals & Materials Soc (TMS), Warrendale, PA, USA, 1991. 457~480

3 Chen QZ, Chu WY, Hsiao JM. In-situ TEM observations of nucleation and bluntness of nanocracks in thin crystals of 310 stainless steel. *Acta Metall Mater*, 1995, 43: 4371

4 Zhang Y, Chu WY, Wang YB. The *in-situ* observation of nanocrack in titanium aluminide. *Science in China*, 1995, 38A: 233

5 Gao KW, Chen QZ, Chu WY. Nucleating and propagating of nanocrack in dislocation free zone in brittle materials. *Science in China*, 1995, 38A: 1501

6 Dewald DK, Lee TC, Robertson IM, et al. Dislocation structures ahead of advancing cracks. *Scri Met*, 1989, 23: 1307~1312

7 Ohr SM. An electron microscope study of crack tip deformation and its impact on the dislocation theory of fracture. *Mater Sci Eng*, 1985, 72: 1

8 Mullins M. Computer simulation of fracture using long range pair potentials. *Acta Metall*, 1984, 32: 381~388

9 Kitagawa H, Nakatani A, Shibutani Y. Molecular dynamics study of crack processes associated with dislocation nucleated at the tip. *Mater Sci Eng*, 1994, A 176: 263

10 Zhang YW, Wang TC, Tang QH. The effect of thermal activation of crack processes at an atomistic crack tip. *J Phys D: Appl Phys*, 1995, 28: 748

11 Finnis MW, Sinclair JE. A simple N-body potential for transition metals. *Phil Mag*, 1984, 50: 45

12 Ackland GJ, Tichy G, Vitek V et al. Simple N-body potentials for the noble metals and nickel. *Phil Mag*, 1987, A56: 735

13 Heermann DW. Computer simulation methods in theoretic physics, 2nd Edition. Berlin: Springer-Verlag, 1990